Towards the improvement of spin-isospin properties in nuclear energy density functionals

Xavier Roca-Maza

Dipartimento di Fisica, Università degli Studi di Milano and INFN, Sezione di Milano,

via Celoria 16, I-20133 Milano, Italy

X. Roca-Maza, G. Colò, and H. Sagawa,
Phys. Rev. **C 86 031306(R) 2012**
H. Liang, P. Zhao, P. Ring, X. Roca-Maza, and J. Meng,
Phys. Rev. **C 86 021302(R) 2012**

Séminaires de Physique Théorique. IPN Orsay. May 28th 2014

General Motivation:

Many-body systems and density functional theories

- Research on quantum mechanical many-body problems is essential in many areas of modern physics
  - electrons in metal, atoms in molecule, electrons in atom, nucleons in nucleus ...
- Density functional theories (DFT) Hohenberg & Kohn:1964
  - reducing the many-body problems formulated in terms of N-particle wave functions to the one-particle level with the local density distribution $\rho(\boldsymbol{r})$
  - no other method achieves comparable accuracy at the same computational cost

General Motivation:

Many-body systems and density functional theories

- Kohn-Sham scheme Kohn & Sham:1965
  - for any interacting system, there exists a **local** single-particle (Kohn-Sham) potential $v_{\mathrm{KS}}(\boldsymbol{r})$, such that the exact ground-state density of the interacting system can be reproduced by non-interacting particles moving in this local potential:
    $\rho(\boldsymbol{r}) = \rho_{\mathrm{KS}}(\boldsymbol{r}) \equiv \sum_i^{\mathrm{occ}} |\phi_i(\boldsymbol{r})|^2$
  - system energy density functional: $E[\rho(\boldsymbol{r})]$

General Motivation:

Nuclear DFT

- Nuclear DFT is a promising tool for investigating the ground-state and excited state properties of nuclei throughout the nuclear chart.
- Since the 1970s, lots of experience have been accumulated in implementing, adjusting, and using the DFT in nuclei.

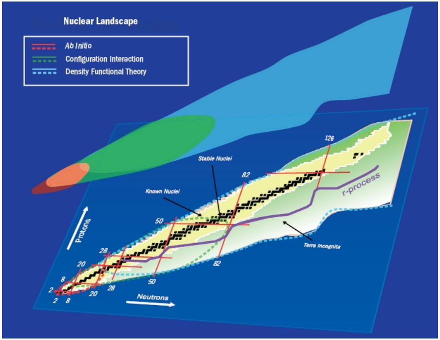

Motivation: Spin-isospin properties

- **H(F)+RPA enables an effective description of the nuclear many-body problem and can be understood as an approximate realization of an EDF**
- **One of the open problems that need to be understood and eventually solved**
  - **Accurate determination** of the **spin-isospin properties** in nuclear effective interactions $\Rightarrow$ **accurate description** of charge exchange excitations such as the **Gamow Teller Resonance**.
- **Gamow Teller**
  - transitions govern electron capture during the core-colapse of supernovæ
  - matrix el. are necessary for the study of **double-β decay** (in neutrinoless double-β decay is crucial for a precise determination of the neutrino mass).
  - matrix el. may be useful in the **calibration of detectors used to measure electron-neutrinos** coming from the Sun

Motivation: Gamow Teller Resonance I

Neither the strength (SR) nor the E_x accurately described in HF+RPA

- SGII[a] ⇒ earliest attempt to give a quantitative description of the GTR
- SkO'[b] ⇒ accurate in ground state finite nuclear properties and improves the GTR
- Relativistic MF and Relativistic HF (PKO1[c]) calculations are also available

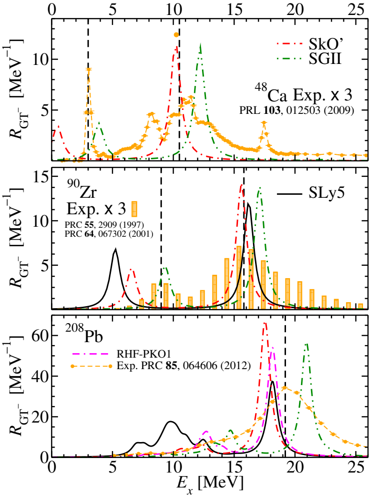

[a]N. Giai and H. Sagawa, Phys. Lett. B **106**, 379 (1981), [b]P.-G. Reinhard et al., Phys. Rev. C **60**, 014316 (1999), [c]H. Liang, N. Van Giai, and J. Meng, Phys. Rev. Lett. **101**, 122502 (2008), SLy5 – E. Chabanat et al., Nucl. Phys. A **635**, 231 (1998); E. Chabanat *et al.*, ibid. **643**, 441 (1998)

Motivation: Gamow Teller Resonance II

Quenching of the strength

- **Experimentally**, the **GTR** exhausts **60–70%** of the **Ikeda sum rule**: $\int [R_{\mathrm{GT}^-}(E) - R_{\mathrm{GT}^+}(E)]dE = 3(N - Z)$
- To **explain** the problem, two possibilities that go beyond RPA correlations have been drawn:
  - the effects of the second-order configuration mixing: **2p-2h correlations**
  - within the quark model, a **n(p)** can become a **p(n)** or a $\Delta^+(\Delta^{++})$ under the action of the GT^- operator and since there is **no Pauli blocking for Δ−h excitations** $\Rightarrow$ it may **contribute to the GTR**.
- The **experimental analysis of ^{90}Zr** $\Rightarrow$ **quenching** (2/3) has to be **mainly attributed to 2p-2h** coupling and not to Δ−isobar effects much smaller [T. Wakasa *et. al.*, Phys. Rev. C **55**, 2909 (1997)].
- E_x **GTR in nuclei** mainly in the region of several **tens of MeV** and the Δ−h states are hundreds of MeV above the GT $\Rightarrow$ **hard to excite the Δ** in the nuclear medium.

New Skyrme interaction with improved spin-isospin properties

Which gs properties are important for describing the E_x^{GTR}?

A recent study[a] on the GTR and the spin-isospin Landau-Migdal parameter G_0' using several Skyrme sets,

- concluded that G_0' **is not the only important quantity** in determining the **excitation energy of the GTR** in nuclei
- **spin-orbit splittings** also influences the GTR

- Empirical indications[b] suggest that $G_0' > G_0 > 0$
- **Not a very common feature** within available Skyrme forces[c]

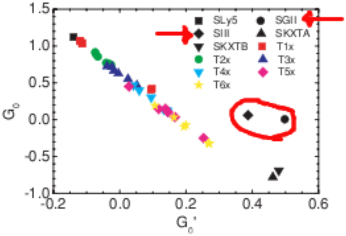

[a] M. Bender, J. Dobaczewski, J. Engel, and W. Nazarewicz, Phys. Rev. C **65**, 054322 (2002); [b] T. Wakasa, M. Ichimura, and H. Sakai, Phys. Rev. C **72**, 067303 (2005); T. Suzuki and H. Sakai, Phys. Lett. B **455**, 25 (1999), [c] Li-Gang Cao, G. Colo, and H. Sagawa, Phys. Rev. C **81**, 044302 (2010)

Why spin-orbit splittings are important?

$E_x^1 \approx \epsilon_{\pi 1g_{7/2}} - \epsilon_{\nu 1g_{9/2}} + \epsilon^1_{\rm ph}$
$E_x^2 \approx \epsilon_{\pi 1g_{9/2}} - \epsilon_{\nu 1g_{9/2}} + \epsilon^2_{\rm ph}$
$\Delta E_x \approx \boldsymbol{\Delta}\epsilon_{\pi \mathbf{1g}} + \Delta\epsilon_{\rm ph}$

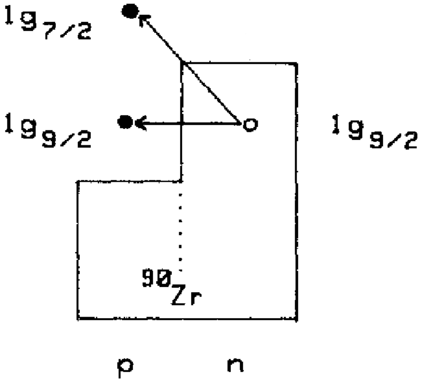

Schematic picture of single-particle transitions involved in the Gamow Teller Resonance of ^{90}Zr. Transitions excited by $\sigma\tau_-$ operator.

F. Osterfeld, Rev. Mod. Phys. **64**, 491 (1992)

Skyrme Model

Hamiltonian[a]

Includes **central tensor terms (J^2 terms)** due to the coupling of tensor and spin and gradients terms and **two spin-orbit parameters** (same as SkO and some SkI forces)

$$\mathcal{H} = \mathcal{K} + \mathcal{H}_0 + \mathcal{H}_3 + \mathcal{H}_{\rm eff} + \mathcal{H}_{\rm fin} + \mathcal{H}_{\rm SO} + \mathcal{H}_{\rm sg} + \mathcal{H}_{\rm Coul}$$

$$\mathcal{K} = \hbar^2 \tau / 2m$$

$$\mathcal{H}_0 = (1/4) t_0 [(2 + x_0)\rho^2 - (2x_0 + 1)(\rho_n^2 + \rho_p^2)]$$

$$\mathcal{H}_3 = (1/24) t_3 \rho^\alpha [(2 + x_3)\rho^2 - (2x_3 + 1)(\rho_n^2 + \rho_p^2)]$$

$$\begin{aligned}\mathcal{H}_{\rm eff} &= (1/8)[t_1(2 + x_1) + t_2(2 + x_2)]\tau\rho \\ &+ (1/8)[t_2(2x_2 + 1) - t_1(2x_1 + 1)](\tau_n\rho_n + \tau_p\rho_p)\end{aligned}$$

$$\begin{aligned}\mathcal{H}_{\rm fin} &= (1/32)[3t_1(2 + x_1) - t_2(2 + x_2)](\nabla\rho)^2 \\ &- (1/32)[3t_1(2x_1 + 1) + t_2(2x_2 + 1)][(\nabla\rho_n)^2 + (\nabla\rho_p)^2]\end{aligned}$$

$$\mathcal{H}_{\rm SO} = (1/2) W_0 \mathbf{J} \cdot \nabla\rho + (1/2) W_0' (\mathbf{J} \cdot_{\mathbf{n}} \nabla\rho_n + \mathbf{J_p} \cdot \nabla\rho_p)$$

$$\mathcal{H}_{\rm sg} = -(1/16)(t_1 x_1 + t_2 x_2)\mathbf{J}^2 + (1/16)(t_1 - t_2)(\mathbf{J_n}^2 + \mathbf{J_p}^2)$$

[a] E. Chabanat et al., Nucl. Phys. A **635**, 231 (1998); E. Chabanat *et al.*, ibid. **643**, 441 (1998)

Fitting Protocol

χ^2 **definition:** $\chi^2 = \frac{1}{N_{\rm data}} \sum_i^{N_{\rm data}} \frac{(\mathcal{O}_i^{\rm theo.} - \mathcal{O}_i^{\rm data})^2}{(\Delta \mathcal{O}_i^{\rm data})^2}$

Landau-Migdal parameters in infinite nuclear matter G_0 and G_0' fixed to **0.15** and **0.35**, respectively, at ρ_0.

Table: Data and *pseudo*-data $\mathcal{O}_i$, adopted errors for the fit $\Delta\mathcal{O}_i$ and selected finite nuclei and EoS.

$\mathcal{O}_i$	$\Delta\mathcal{O}_i$	
B	1.00 MeV	^{40,48}Ca, ^{90}Zr, ^{132}Sn and ^{208}Pb
r_c	0.01 fm	^{40,48}Ca, ^{90}Zr and ^{208}Pb
$\Delta E_{\rm SO}$	$0.04\times\mathcal{O}_i$	$\pi 1g$ in ^{90}Zr and $\pi 2f$ in ^{208}Pb
$e_n(\rho)$	$0.20\times\mathcal{O}_i$	R. B. Wiringa *et al.*, PRC **38**, 1010 (1988)

Skyrme Aizu Milano interaction: SAMi

Parameter set and nuclear matter properties:

Table: SAMi parameter set and saturation properties with the estimated standard deviations inside parenthesis

	value(σ)			value(σ)	
t_0	$-1877.75(75)$	MeV fm^3	ρ_∞	0.159(1)	fm^{-3}
t_1	475.6(1.4)	MeV fm^5	e_∞	$-15.93(9)$	MeV
t_2	$-85.2(1.0)$	MeV fm^5	$m^*_{\rm IS}$	0.6752(3)	
t_3	10219.6(7.6)	MeV fm$^{3+3\alpha}$	$m^*_{\rm IV}$	0.664(13)	
x_0	0.320(16)		J	28(1)	MeV
x_1	$-0.532(70)$		L	44(7)	MeV
x_2	$-0.014(15)$		K_∞	245(1)	MeV
x_3	0.688(30)		G_0	0.15	(fixed)
W_0	137(11)		G_0'	0.35	(fixed)
W_0'	42(22)				
α	0.25614(37)				

SAMi: spin and spin-isospin instabilities in NM

Imposing that spin and isospin dof at the Fermi surface are stable under generalized deformations [S.-O. Bäckman *et al.*, Nucl. Phys. A **321**, 10 (1979)]

$$1 + G_0 > 0 \qquad\qquad 1 + G_0' > 0$$

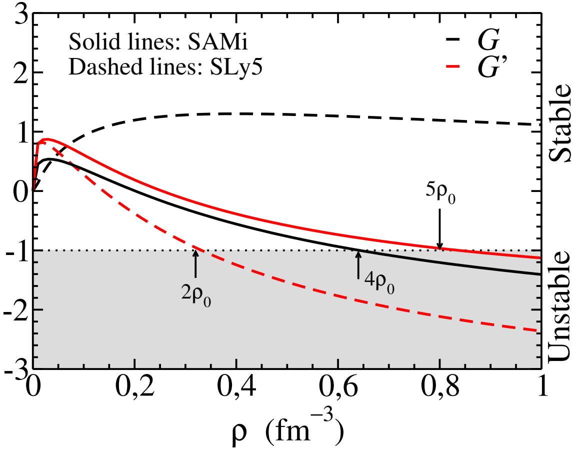

Results

Equation of State: SAMi vs *ab*–initio calculations

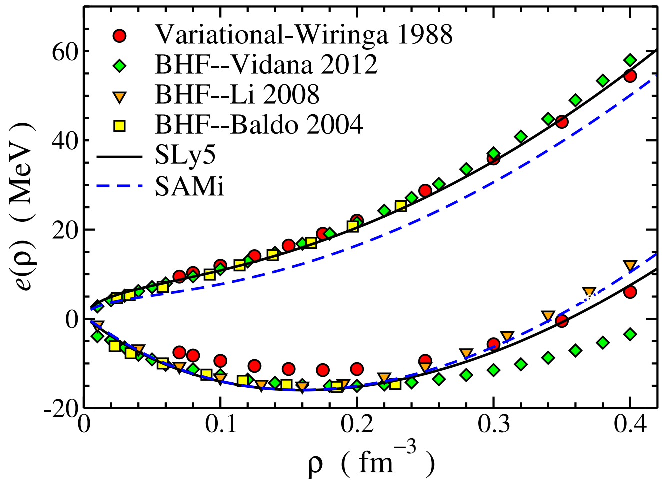

Figure: Neutron and symmetric matter EoS as predicted by the HF SAMi (dashed line) and SLy5 (solid line) interactions and by the benchmark microscopic calculations of R. B. Wiringa *et al.*, PRC **38**, 1010 (1988) (circles). State-of-the-art BHF calculations are shown by diamonds I. Vidaña, private communication, triangles Z. H. Li *et al.*, Phys. Rev. C **77**, 034316 (2008) and squares M. Baldo *et al.*, Nucl. Phys. A **736**, 241 (2004).

Results

Finite Nulcei: spherical double-magic nuclei

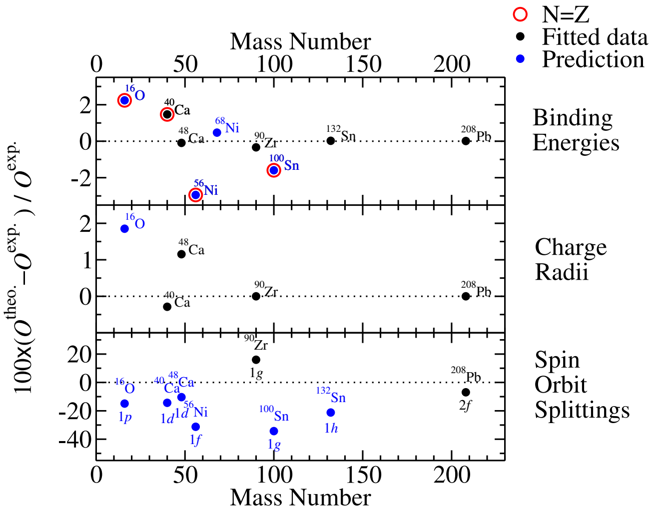

Figure: Finite nuclei properties as predicted by the HF SAMi (black circles) and some predictions (blue circles) for spherical double-magic nuclei. Experimental data taken from Refs. G. Audi *et al.*, NPA **729**, 337 (2003), I. Angeli, ADNDT **87**, 185 (2004), M. Zalewski *et al.*, PRC **77**, 024316 (2008)

Results

Giant Monopole and Dipole Resonances in ^{208}Pb

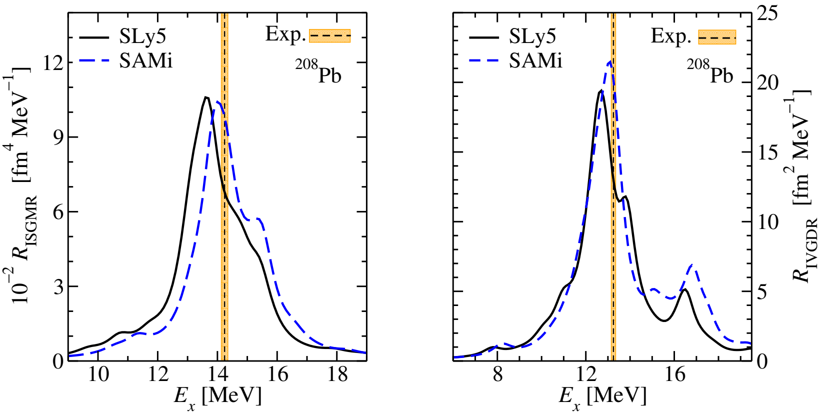

Figure: Strength function at the relevant excitation energies in ^{208}Pb as predicted by SLy5 and the SAMi interaction for GMR and GDR. A Lorentzian smearing parameter equal to 1 MeV is used. Experimental data for the centroid energies are also shown: $E_c(GMR) = 14.24 \pm 0.11$ MeV [D. H. Youngblood, et al., Phys. Rev. Lett. **82**, 691 (1999)] and $E_c(GDR) = 13.25 \pm 0.10$ MeV [N. Ryezayeva et al., Phys. Rev. Lett. **89**, 272502 (2002)].

Results

Gamow Teller Resonance in ^{48}Ca, ^{90}Zr and ^{208}Pb

Operator:
$\sum_{i=1}^{A} \sigma(i)\tau_{\pm}(i)$

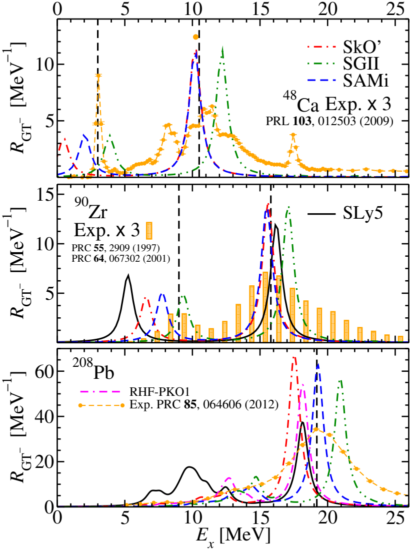

Figure: Gamow Teller strength distributions in ^{48}Ca (upper panel), ^{90}Zr (middle panel) and ^{208}Pb (lower panel) as measured in the experiment [T. Wakasa *et al.*, Phys. Rev. C **55**, 2909 (1997), K. Yako *et al.*, Phys. Rev. Lett. **103**, 012503 (2009), A. Krasznaborkay *et al.*, Phys. Rev. C **64**, 067302 (2001), H. Akimune *et al.*, Phys. Rev. C **52**, 604 (1995) and T. Wakasa et al., Phys. Rev. C **85**, 064606 (2012)] and predicted by SLy5, SkO', SGII and SAMi forces.

Results

Spin Dipole Resonances in ^{90}Zr and ^{208}Pb

Operator:

$$\sum_{i=1}^{A}\sum_{M}\tau_{\pm}(i)r_i^L\left[Y_L(\hat{r}_i)\otimes\sigma(i)\right]_{JM}$$

Sum Rule:

$$\int[R_{\mathrm{SD}^-}(E)-R_{\mathrm{SD}^+}(E)]\mathrm{d}E=\frac{9}{4\pi}\left(N\langle r_n^2\rangle-Z\langle r_p^2\rangle\right)$$

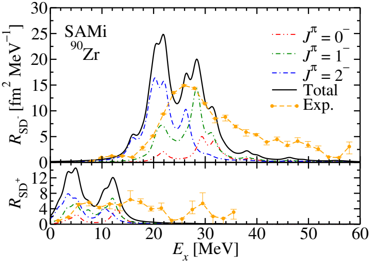

Figure: Spin Dipole strength distributions in ^{90}Zr as a function of the excitation energy E_x in the τ_- channel (upper panel) and τ_+ channel (lower panel) measured in the experiment [K. Yako *et al.*, Phys. Rev. C **74**, 051303(R) (2006)] and predicted by SAMi. Multipole decomposition is also shown. A Lorentzian smearing parameter equal to 2 MeV is used.

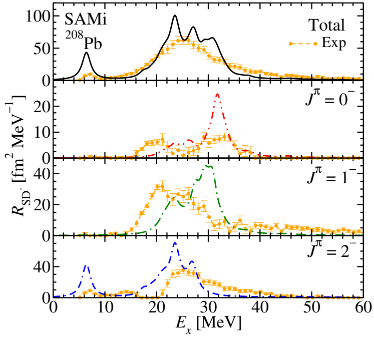

Figure: SDR strength distributions for ^{208}Pb in the τ_- channel from experiment [T. Wakasa *et al.*, Phys. Rev. C **85**, 064606 (2012)] and SAMi calculations. Total and multipole decomposition of the SDR strength are shown: total (upper panel), $J^\pi = 0^-$ (middle-upper panel), $J^\pi = 1^-$ (middle-lower panel) and $J^\pi = 2^-$ (lower panel). A Lorentzian smearing parameter equal to 2 MeV is used.

Conclusions:

- we have **successfully determined a new Skyrme** energy density functional which **accounts** for the most relevant quantities in order to improve the description of **charge-exchange nuclear resonances**:
  - the **hierarchy** and **positive values** of the spin and spin-isospin Landau-Migdal parameters G_0 **and** G_0'
  - the **proton spin-orbit splittings** of different **high angular momenta** single-particle levels
- the **GTR** in ^{48}Ca and the **GTR**, **IAR**, and **SDR** in ^{90}**Zr** and ^{208}**Pb** are predicted with **good accuracy by SAMi**
- **SAMi** does **not deteriorate** the description of other **nuclear observables**
- **applicability in nuclear physics and astrophysics**

Localized form of Fock terms in nuclear covariant density functional theory

Covariant density functional theory – RH theory

- The covariant version of DFT takes into account Lorentz symmetry.
- CDFT in Hartree level (RH/RMF theory) has received wide attention due to its successful description of lots of nuclear phenomena.
  Serot:1986, Ring:1996, Vretenar:2005, Meng:2006, Paar:2007, Nikšić:2011
  - ⋆ spin-orbit splittings
  - ⋆ EoS in symmetric and asymmetric nuclear matter
  - ⋆ ground-state properties of finite spherical and deformed nuclei
  - ⋆ collective rotational and vibrational excitations
  - ⋆ low-lying spectra of transitional nuclei involving quantum phase transitions
  - ⋆ ......

Covariant density functional theory – RH theory

Common problems in the isovector channels

- Difficult to disentangle the isovector-scalar (δ) and isovector-vector (ρ) channels, unless a tuning is performed based on selected microscopic calculations. Roca-Maza:2011
- Nuclear spin-isospin resonances, e.g., GTR and SDR, cannot be described in a fully self-consistent way.

Covariant density functional theory – RHF theory

CDFT in Hartree-Fock level (RHF theory)

- ⋆ several attempts to include the Fock term in the relativistic framework

  Bouyssy:1985,1987, Bernardos:1993, Marcos:2004

- ⋆ DDRHF theory achieved quantitative descriptions of binding energies and radii

  Long, Giai, Meng, *PLB* **640**, 150 (2006); Long, Sagawa, Giai, Meng, *PRC* **76**, 034314 (2007);
  Long, Sagawa, Meng, Giai, *EPL* **82**, 12001 (2008); Long, Ring, Giai, Meng, *PRC* **81**, 024308 (2010)

- ⋆ effective mass splitting in asymmetric nuclear matter can be described naturally

  Long, Giai, Meng, *PLB* **640**, 150 (2006)

Covariant density functional theory – RHF theory

- ⋆ nuclear spin-isospin resonances can be described in a fully self-consistent way
  HL, Giai, Meng, *PRL* **101**, 122502 (2008); HL, Giai, Meng, *PRC* **79**, 064316 (2009);
  HL, Zhao, Meng, *PRC* **85**, 064302 (2012)

- RHF includes **non-local** potentials $v_{\mathrm{HF}}(\boldsymbol{r}, \boldsymbol{r}')$
- RHF is much more complicated than RH theory.
- The computational cost is too expensive for including paring, deformation, projection, cranking, ...

To construct RH functionals from RHF scheme

It is therefore desirable

- to find a covariant density functional based on only local potentials, yet keeping the merits of the exchange terms
- Possible/promising solution: construct RH functionals from RHF scheme
  - ⋆ take the constraints introduced by exchange terms of RHF scheme into account
- We start from an important observation: RHF functional PKO2 [Long:2008]
  - ⋆ well describes the neutron-proton Dirac mass splitting in asymmetric nuclear matter and nuclear spin-isospin resonances
  - ⋆ only includes σ-, ω-, ρ-mesons, but not π-meson
  - ⋆ masses of mesons are heavy $\Rightarrow$ zero-range approximation is reasonable
  - ⋆ Fierz transformation: Fock terms $\Rightarrow$ local Hartree terms

In the present work

- To construct RH functional from RHF scheme by the following procedure
  - ⋆ start with RHF parametrization PKO2
  - ⋆ perform the zero-range reduction
  - ⋆ perform the Fierz transformation

- With such RH functional thus obtained, to investigate
  - ⋆ proton-neutron Dirac mass splitting in neutron matter
  - ⋆ Gamow-Teller and spin-dipole resonances

Goal(s)

- To verify whether the important effects of exchange terms can be maintained by the mapping from RHF functional to RH functional.

Covariant density functional theory – RHF theory

- Effective Lagrangian density Bouyssy:1987, Long:2006

$$\mathcal{L} = \bar{\psi}\left[i\gamma^\mu\partial_\mu - M - g_\sigma\sigma - \gamma^\mu\left(g_\omega\omega_\mu + g_\rho\vec{\tau}\cdot\vec{\rho}_\mu + e\frac{1-\tau_3}{2}A_\mu\right)\right]\psi$$
$$+\frac{1}{2}\partial^\mu\sigma\partial_\mu\sigma - \frac{1}{2}m_\sigma^2\sigma^2 - \frac{1}{4}\Omega^{\mu\nu}\Omega_{\mu\nu} + \frac{1}{2}m_\omega^2\omega_\mu\omega^\mu - \frac{1}{4}\vec{R}_{\mu\nu}\cdot\vec{R}^{\mu\nu} + \frac{1}{2}m_\rho^2\vec{\rho}^\mu\cdot\vec{\rho}_\mu - \frac{1}{4}F^{\mu\nu}F_{\mu\nu} \tag{1}$$

- System Hamiltonian

$$\mathcal{H} = \mathcal{T}^{00} = \frac{\partial\mathcal{L}}{\partial\dot{\phi}_i}\dot{\phi}_i - \mathcal{L} \tag{2}$$

- Ground-state trial wave function

$$|\Phi_0\rangle = \prod_a c_a^\dagger |0\rangle \tag{3}$$

- Energy functional of the system

$$E = \langle\Phi_0| H |\Phi_0\rangle = E_k + E_\sigma^D + E_\omega^D + E_\rho^D + E_A^D + E_\sigma^E + E_\omega^E + E_\rho^E + E_A^E \tag{4}$$

Zero-range reduction

- Yukawa propagators of the mesons

$$D_i(\boldsymbol{r},\boldsymbol{r}') = \frac{1}{4\pi}\frac{e^{-m_i|\boldsymbol{r}-\boldsymbol{r}'|}}{|\boldsymbol{r}-\boldsymbol{r}'|}, \qquad D_i(\boldsymbol{q}) = \frac{1}{m_i^2+\boldsymbol{q}^2} \tag{5}$$

for $m_i \gg q$,

$$D_i(\boldsymbol{q}) \approx \frac{1}{m_i^2} - \frac{\boldsymbol{q}^2}{m_i^4} + \cdots \quad \Rightarrow \quad D_i(\boldsymbol{r},\boldsymbol{r}') \approx \frac{1}{m_i^2}\delta(\boldsymbol{r}-\boldsymbol{r}') \tag{6}$$

within the zero-order approximation.

- Zero-range reduction of meson-nucleon couplings

$$\alpha_S = -\frac{g_\sigma^2}{m_\sigma^2}, \qquad \alpha_V = \frac{g_\omega^2}{m_\omega^2}, \qquad \alpha_{tV} = \frac{g_\rho^2}{m_\rho^2}, \tag{7}$$

Fierz transformation (I)

- Dirac matrices form a complete system

$$O^S = 1, O^V = \gamma^\mu, O^T = \sigma^{\mu\nu}, O^{PS} = \gamma^5, O^{PV} = \gamma^5\gamma^\mu$$

so that any one can be expressed as a linear superposition of variants with a changed sequence of spinors,

$$(\bar{a}O^i d)(\bar{c}O_i b) = \sum_k c_{ik}(\bar{a}O^k b)(\bar{c}O_k d), \tag{8}$$

with the coefficients c_{ik} in the so-called Fierz table Fierz:1937, Okun:1982, Sulaksono:2003

$$\begin{array}{cccccc} & S & V & T & PS & PV \\ S & \frac{1}{4} & \frac{1}{4} & \frac{1}{8} & \frac{1}{4} & -\frac{1}{4} \\ V & 1 & -\frac{1}{2} & 0 & -1 & -\frac{1}{2} \\ T & 3 & 0 & -\frac{1}{2} & 3 & 0 \\ PS & \frac{1}{4} & -\frac{1}{4} & \frac{1}{8} & \frac{1}{4} & \frac{1}{4} \\ PV & -1 & -\frac{1}{2} & 0 & 1 & -\frac{1}{2} \end{array} \tag{9}$$

Fierz transformation (II)

- Fierz transformation: from α^{HF} to α^{H}

$$\alpha_S^{\mathrm{H}} = +\frac{7}{8}\alpha_S^{\mathrm{HF}} - \frac{4}{8}\alpha_V^{\mathrm{HF}} - \frac{12}{8}\alpha_{tV}^{\mathrm{HF}} \tag{10a}$$

$$\alpha_{tS}^{\mathrm{H}} = -\frac{1}{8}\alpha_S^{\mathrm{HF}} - \frac{4}{8}\alpha_V^{\mathrm{HF}} + \frac{4}{8}\alpha_{tV}^{\mathrm{HF}} \tag{10b}$$

$$\alpha_V^{\mathrm{H}} = -\frac{1}{8}\alpha_S^{\mathrm{HF}} + \frac{10}{8}\alpha_V^{\mathrm{HF}} + \frac{6}{8}\alpha_{tV}^{\mathrm{HF}} \tag{10c}$$

$$\alpha_{tV}^{\mathrm{H}} = -\frac{1}{8}\alpha_S^{\mathrm{HF}} + \frac{2}{8}\alpha_V^{\mathrm{HF}} + \frac{6}{8}\alpha_{tV}^{\mathrm{HF}} \tag{10d}$$

$$\alpha_T^{\mathrm{H}} = -\frac{1}{16}\alpha_S^{\mathrm{HF}} \tag{10e}$$

$$\alpha_{tT}^{\mathrm{H}} = -\frac{1}{16}\alpha_S^{\mathrm{HF}} \tag{10f}$$

$$\alpha_{PS}^{\mathrm{H}} = -\frac{1}{8}\alpha_S^{\mathrm{HF}} + \frac{4}{8}\alpha_V^{\mathrm{HF}} + \frac{12}{8}\alpha_{tV}^{\mathrm{HF}} \tag{10g}$$

$$\alpha_{tPS}^{\mathrm{H}} = -\frac{1}{8}\alpha_S^{\mathrm{HF}} + \frac{4}{8}\alpha_V^{\mathrm{HF}} - \frac{4}{8}\alpha_{tV}^{\mathrm{HF}} \tag{10h}$$

$$\alpha_{PV}^{\mathrm{H}} = +\frac{1}{8}\alpha_S^{\mathrm{HF}} + \frac{2}{8}\alpha_V^{\mathrm{HF}} + \frac{6}{8}\alpha_{tV}^{\mathrm{HF}} \tag{10i}$$

$$\alpha_{tPV}^{\mathrm{H}} = +\frac{1}{8}\alpha_S^{\mathrm{HF}} + \frac{2}{8}\alpha_V^{\mathrm{HF}} - \frac{2}{8}\alpha_{tV}^{\mathrm{HF}} \tag{10j}$$

Dirac mass and its isospin splitting

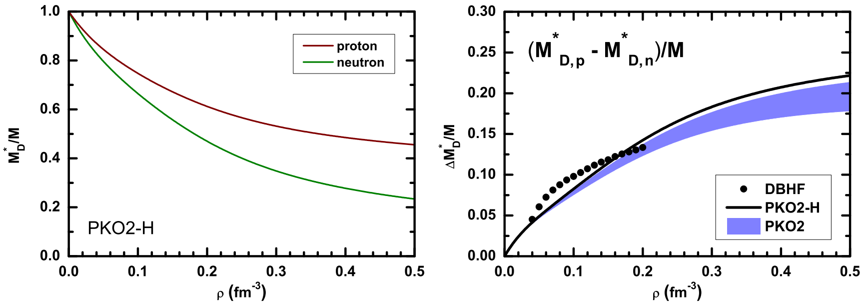

DBHF: van Dalen, *et al.*, *EPJA* **31**, 29 (2007)

- It is found that $M^*_{D,p} > M^*_{D,n}$.
- The splitting behavior in neutron matter is consistent with the prediction of the Dirac-Brueckner-Hartree-Fock (DBHF) calculations.
- The constraints introduced by the Fock terms of the RHF scheme into the tS channel of the present density functional are straight forward and quite robust.

Gamow-Teller resonances

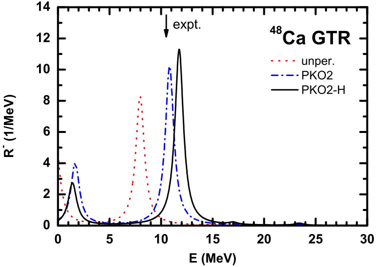

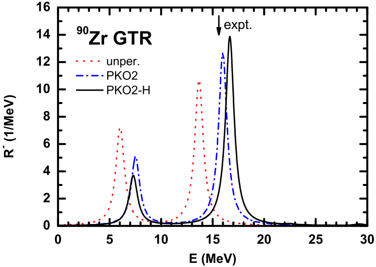

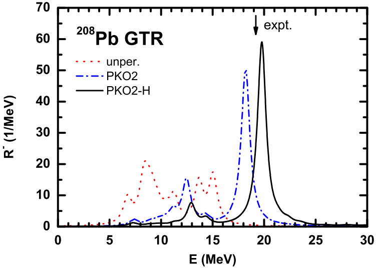

- GTR excitation energies can be well reproduced by the *ph* residual interactions of PKO2-H.
- The present results are similar as those by the original RHF+RPA.
- The difference is due to the zero-range approximation.

Gamow-Teller resonances in ^{208}Pb

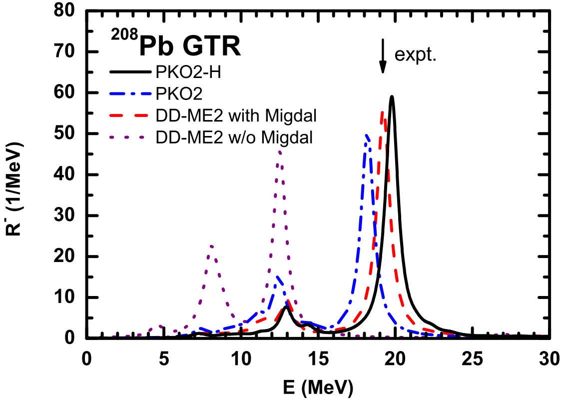

- It is fitted for DD-ME2 by adjusting the Migdal term.

RHF+RPA: HL, Giai, Meng, *PRL* **101**, 122502 (2008)

RH+RPA: Paar, Nikšić, Vretenar, Ring, *PRC* **69**, 054303 (2004)

Physical mechanisms of GTR

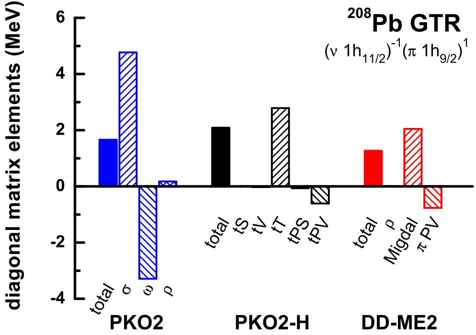

- In RHF+RPA (PKO2), σ- and ω-mesons play the most important role in determining the properties of GTR via the exchange terms.
- In the RHF equivalent RPA (PKO2-H), tT and tPV channels are most important, their coupling strengths are intrinsically determined by Fierz transformation.
- In conventional RH+RPA (DD-ME2), the free π residual interaction is attractive and the Migdal term is repulsive by fitting to experimental data.

Spin-dipole resonances

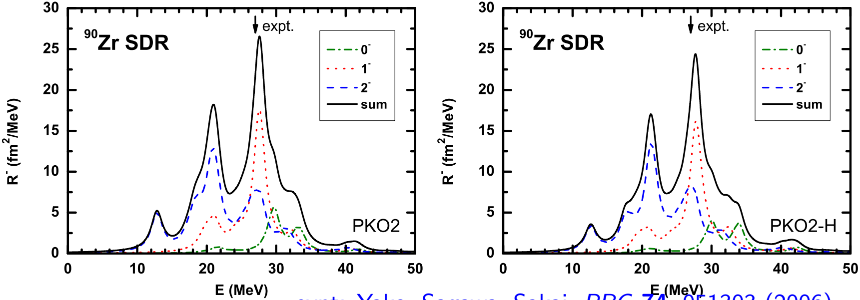

expt: Yako, Sagawa, Sakai, *PRC* **74**, 051303 (2006)

- Not only the total strengths but also the individual contribution from different spin-parity J^π components are almost identical.
- The energy hierarchy $E(2^-) < E(1^-) < E(0^-)$ can be obtained in the present RPA calculations in the local scheme.
- Therefore, the constraints introduced by the Fock terms of the RHF scheme into the *ph* residual interactions seem to be aslo robust.

Summary and Perspectives

Summary

★ A new method is proposed to take into account the Fock terms in local covariant density functionals.

✓ The advantages of existing RH functionals can be maintained, while the problems in the isovector channel can be solved.

- ⋆ The neutron-proton Dirac mass splitting in asymmetric nuclear matter is in a very good agreement with the prediction of DBHF.
- ⋆ The properties of GTR and SDR can be reproduced in a natural way.

Perspectives

- This opens a new door for the development of nuclear local covariant density functionals with better isoscalar and isovector properties in the future.

Covariance analysis

Covariance analysis: χ^2 test

Observables $\mathcal{O}$ are used to calibrate the parameters $\mathbf{p}$ of a given model. The optimum parametrization $\mathbf{p}_0$ is determined by a least-squares fit with the global quality measure,

$$\chi^2(\mathbf{p}) = \sum_{\imath=1}^{m} \left(\frac{\mathcal{O}_\imath^{\text{theo.}} - \mathcal{O}_\imath^{\text{ref.}}}{\Delta \mathcal{O}_\imath^{\text{ref.}}} \right)^2$$

Assuming that the χ^2 is a well behaved (analytical) function in the vicinity of the minimum and that can be approximated by an hyper-parabola,

$$\begin{aligned} \chi^2(\mathbf{p}) - \chi^2(\mathbf{p}_0) &\approx \frac{1}{2} \sum_{\imath,\jmath}^{n} (p_\imath - p_{0\imath}) \partial_{p_\imath} \partial_{p_\jmath} \chi^2 (p_\jmath - p_{0\jmath}) \\ &\equiv \sum_{\imath,\jmath}^{n} (p_\imath - p_{0\imath}) \mathcal{M}_{\imath\jmath} (p_\jmath - p_{0\jmath}) \end{aligned}$$

where $\mathcal{M}$ is the curvature matrix.

Covariance analysis: χ^2 test

$\mathcal{M}$ provides us access to estimate the errors between predicted observables ($A(\mathbf{p})$),

$$\Delta\mathcal{A} = \sqrt{\sum_{\imath}^{n} \partial_{p_\imath} A \mathcal{E}_{\imath\imath} \partial_{p_\imath} A} \tag{11}$$

$\mathcal{E} = \mathcal{M}^{-1}$ and the correlations between predicted observables,

$$c_{AB} \equiv \frac{C_{AB}}{\sqrt{C_{AA} C_{BB}}} \tag{12}$$

where,

$$C_{AB} = \overline{(A(\mathbf{p}) - \overline{A})(B(\mathbf{p}) - \overline{B})} \approx \sum_{\imath\jmath}^{n} \partial_{p_\imath} A \mathcal{E}_{\imath\jmath} \partial_{p_\jmath} B$$

Covariance analysis: SLy5-min as an example

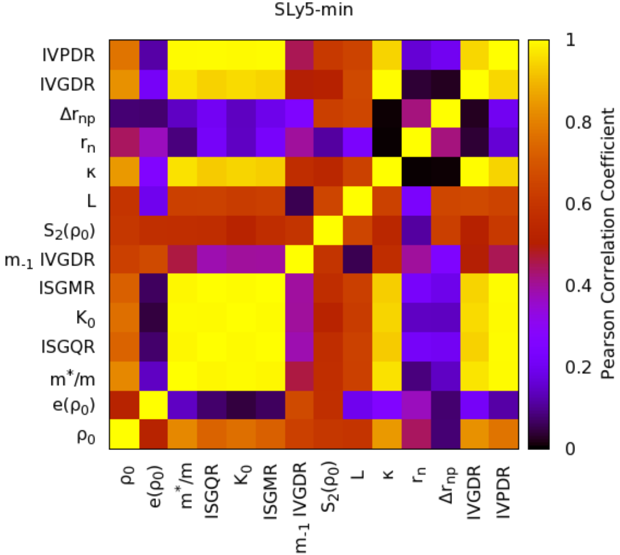

Covariance analysis: SLy5-min as an example

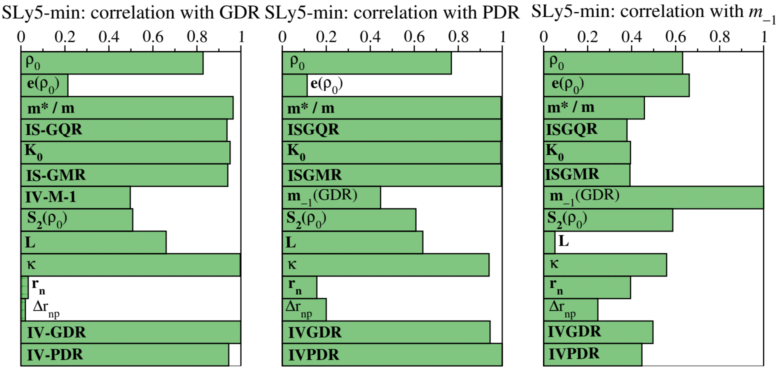

Figure: Pearson product-moment correlation coefficient for the IVGDR (left panel), IVPDR (middle panel) and m_{-1}(IVGDR) (right panel) with all other studied properties as predicted by the covariance analysis of SLy5.

Thank you for your attention!